

Online Quench-Flow Electrospray Ionization Fourier Transform Ion Cyclotron Resonance Mass Spectrometry for Elucidating Kinetic and Chemical Enzymatic Reaction Mechanisms

David J. Clarke,* Adam A. Stokes, Pat Langridge-Smith, and C. Logan Mackay

SIRCAMS, School of Chemistry, University of Edinburgh, West Mains Road, Edinburgh, EH9 3JJ, U.K.

We have developed an automated quench-flow microreactor which interfaces directly to an electrospray ionization (ESI) mass spectrometer. We have used this device in conjunction with ESI Fourier transform ion cyclotron resonance mass spectrometry (FTICR MS) to demonstrate the potential of this approach for studying the mechanistic details of enzyme reactions. For the model system chosen to test this device, namely, the pre-steady-state hydrolysis of *p*-nitrophenyl acetate by the enzyme chymotrypsin, the kinetic parameters obtained are in good agreement with those in the literature. To our knowledge, this is the first reported use of online quench-flow coupled with FTICR MS. Furthermore, we have exploited the power of FTICR MS to interrogate the quenched covalently bound enzyme intermediate using top-down fragmentation. The accurate mass capabilities of FTICR MS permitted the nature of the intermediate to be assigned with high confidence. Electron capture dissociation (ECD) fragmentation allowed us to locate the intermediate to a five amino acid section of the protein—which includes the known catalytic residue, Ser₁₉₅. This experimental approach, which uniquely can provide both kinetic and chemical details of enzyme mechanisms, is a potentially powerful tool for studies of enzyme catalysis.

The introduction of electrospray ionization (ESI) and matrix-assisted laser desorption ionization (MALDI) in the mid-1980s has made mass spectrometry (MS) an essential tool in many branches of protein chemistry.^{1,2} As a result, the use of MS as a detection technique in enzyme kinetic studies has become more widespread over the past few years.^{3,4} This technique was first employed in 1989 by Lee et al., who performed online continuous flow experiments using a triple-quadrupole mass spectrometer to directly monitor the activity of both lactase and α -chymotrypsin.⁵ Their experiments allowed the determination of Michaelis–Menten

kinetic parameters (K_M and V_{max}) which were consistent with results obtained using conventional steady-state kinetic analyses. The use of MS over traditional spectroscopic detection techniques has several potential advantages. First, because virtually all enzymatic conversions (with the exception of epimerases and racemases) result in a change in mass, natural substrates can be used in monitoring enzyme-catalyzed reactions. This obviates the requirement for chromophoric or radiolabeled substrates. Bothner et al. have highlighted this advantage by analyzing several enzyme-catalyzed hydrolysis reactions, demonstrating significant differences in the kinetics between natural and chromophore-labeled substrates.⁶ Second, this experimental approach takes advantage of the high sensitivity and selectivity inherent in modern mass spectrometers, when compared to spectrophotometric detectors. Additionally, MS detection affords the user the ability to observe multiple species simultaneously. These advantages allow the kinetic analysis of enzymes which would be impossible to study using spectrophotometric detectors. For example, Leary and co-workers have successfully used MS to characterize the kinetics of enzymatic sulfate and phosphate group transfer.^{7–10}

The interfacing of a rapid mixing system, such as a stopped-or quench-flow apparatus, with a mass spectrometer was first proposed in 1997.¹¹ Theoretically, if mixing systems operate at sufficiently high temporal resolution (typically milliseconds for enzyme reactions), this approach allows the direct detection of the relative concentrations of not only reactants and products but also transient intermediates. Therefore, this combination promises the exciting possibilities of determining both *kinetic* mechanisms (and the accompanying kinetic parameters) as well as *chemical* mechanisms (the chemical nature of catalysis and stepwise reaction pathways).

To date time-resolved mass spectroscopy has been achieved using a variety of instrumentation, including electron impact

* To whom correspondence should be addressed. Phone: +44-131-651-3034. E-mail: dave.clarke@ed.ac.uk.

- (1) Fenn, J. B.; Mann, M.; Meng, C. K.; Wong, S. F.; Whitehouse, C. M. *Science* **1989**, *246*, 64–71.
- (2) Karas, M.; Hillenkamp, F. *Anal. Chem.* **1988**, *60*, 2299–2301.
- (3) Liesener, A.; Karst, U. *Anal. Bioanal. Chem.* **2005**, *382*, 1451–1464.
- (4) Shipovskov, S.; Reimann, C. T. *Analyst* **2007**, *132*, 397–402.
- (5) Lee, E. D.; Muck, W.; Henion, J. D.; Covey, T. R. *J. Am. Chem. Soc.* **1989**, *111*, 4600–4604.

- (6) Bothner, B.; Chavez, R.; Wei, J.; Strupp, C.; Phung, Q.; Schneemann, A.; Siuzdak, G. *J. Biol. Chem.* **2000**, *275*, 13455–13459.
- (7) Pi, N.; Armstrong, J. I.; Bertozzi, C. R.; Leary, J. A. *Biochemistry* **2002**, *41*, 13283–13288.
- (8) Pi, N.; Leary, J. A. *J. Am. Soc. Mass Spectrom.* **2004**, *15*, 233–243.
- (9) Pi, N.; Hoang, M. B.; Gao, H.; Mougous, J. D.; Bertozzi, C. R.; Leary, J. A. *Anal. Biochem.* **2005**, *341*, 94–104.
- (10) Gao, H.; Leary, J. A. *J. Am. Soc. Mass Spectrom.* **2003**, *14*, 173–181.
- (11) Northrop, D. B.; Simpson, F. B. *Bioorg. Med. Chem.* **1997**, *5*, 641–644.

MS^{12,13} and MALDI-MS.¹⁴ However, rapid mixing systems are best suited in combination with ESI-MS, an approach which allows a direct “online” link between the solution phase reaction mixture and the ESI-MS inlet. This soft-ionization technique has been widely used to detect analytes ranging from small molecules to peptides and large proteins, and it has also been successfully utilized to monitor noncovalent enzyme–substrate interactions.^{9,15} Two early reports using ESI quench-flow MS detail the observation of transient intermediates bound to the iron binding glycopeptide bleomycin.^{16,17} These species displayed half-lives on the order of several seconds. More recently, the temporal resolution of rapid mixing MS has been improved to some tens of milliseconds through the use of miniaturized mixers, capillaries, and ESI sources.^{15,18–20}

The first study in which time-resolved ESI-MS was used to determine the pre-steady-state kinetic parameters of an enzymatic reaction was published in 1998.²¹ The authors monitored the appearance of a transient covalent enzyme intermediate within the active site of a mutant xylanase enzyme from *Bacillus circulans*. Data was collected using a basic mixing system attached directly to an ESI source, and the resulting kinetic parameters were in excellent agreement with those obtained using stopped-flow UV–vis spectroscopy. More recently, this research group has developed an elegant custom-built capillary mixer attachment which featured an adjustable reaction chamber volume.²² This device allowed measurements with low-millisecond resolution and has successfully been used in conjunction with a triple-quadrupole MS to study the steady-state and pre-steady-state kinetics of chymotrypsin.²³

An alternative approach using an “off-line” rapid quench step is generally more time-consuming than “online” systems. However, it is technically simpler and allows greater flexibility in the workup of each quenched reaction. For example, high-performance liquid chromatography (HPLC) separation, desalting, or chemical digest can be employed prior to MS analysis. Furthermore, an “off-line” workflow does not limit the choice of MS instrumentation to ESI, and it has been effectively using in conjunction with both MALDI and desorption/ionization on silicon (DIOS) desorption/ionization instruments for analysis of pre-steady-state enzyme kinetics.^{14,24–26} Kelleher and co-workers have successfully used “off-line” rapid-quench technology in conjunction

with high-resolution Fourier transform MS (FTMS) in order to characterize the mechanism of a nonribosomal peptide synthetase (NRPS).^{27,28} Several transient enzyme-bound intermediates in the enzymatic production of yersiniabactin were kinetically resolved “off-line” using a commercial rapid-quench instrument. These samples were then processed by chemical cleavage and HPLC before analysis on an ESI-Q-FTMS instrument. The percentage occupancies of the multiple active sites were calculated at various time points, allowing the authors to deduce the rate of accumulation of specific intermediates and propose a general kinetic model for NRPS systems.

The high resolving power of FTMS is ideally suited to the detection and interrogation of covalently bound enzyme intermediates. Mass resolution of 100 000–500 000 is achievable using these instruments, allowing the detection of a 1 Da mass shift (Δm) at ~30 kDa with high confidence. Moreover, the inherent high sensitivity permits detection of low-abundance intermediates.²⁹ In addition, top-down tandem MS fragmentation methodologies, available using FTMS, enable precise localization of these modifications on the polypeptide chain.^{30–33} We have previously demonstrated the utility of FTMS in interrogating the nature and location of intermediates in the catalytic cycle of cysteine-dependent peroxiredoxins.³⁴

In the work presented here we show that FTMS can be utilized for pre-steady-state analysis of enzyme mechanisms. We have built an automated “online” rapid-quench microreactor which operates at low-millisecond temporal resolution. This device is interfaced directly with a commercial ESI Fourier transform ion cyclotron resonance (ESI-FTICR) MS instrument (Bruker Daltonics). Analogous to Wilson and Konermann, we have used the chymotrypsin-catalyzed hydrolysis of *p*-nitrophenyl acetate (*p*-NPA) as a model system.²³ Monitoring this reaction by FTICR MS, we were able to directly observe the appearance of the enzyme-bound acyl-intermediate and deduce pre-steady-state rate constants which are in agreement with previous MS- and optical-based studies. Furthermore, we have exploited the ultrahigh resolving power and mass accuracy of FTICR, to analyze the quenched enzyme-bound acyl-intermediate by top-down fragmentation. Using electron capture dissociation we demonstrate that it is possible to locate the quenched transient acyl modification at position Ser₁₉₅. Our results highlight the advantages of using an “online” ESI quench-flow FTMS system, which can provide valuable insight into both kinetic and chemical mechanisms of enzymatic reactions.

- (12) Northrop, D. B.; Simpson, F. B. *Arch. Biochem. Biophys.* **1998**, *352*, 288–292.
- (13) Orsnes, H.; Graf, T.; Degn, H.; Murray, K. K. *Anal. Chem.* **2000**, *72*, 251–254.
- (14) Houston, C. T.; Taylor, W. P.; Widlanski, T. S.; Reilly, J. P. *Anal. Chem.* **2000**, *72*, 3311–3319.
- (15) Li, Z.; Sau, A. K.; Shen, S.; Whitehouse, C.; Baasov, T.; Anderson, K. S. *J. Am. Chem. Soc.* **2003**, *125*, 9938–9939.
- (16) Sam, J. W.; Tang, X. J.; Magliozzo, R. S.; Peisach, J. J. *Am. Chem. Soc.* **1995**, *117*, 1012–1018.
- (17) Sam, J. W.; Tang, X. J.; Peisach, J. J. *Am. Chem. Soc.* **1994**, *116*, 5250–5256.
- (18) Paiva, A. A.; Tilton, R. F., Jr.; Crooks, G. P.; Huang, L. Q.; Anderson, K. S. *Biochemistry* **1997**, *36*, 15472–15476.
- (19) Kolakowski, B. M.; Simmons, D. A.; Konermann, L. *Rapid Commun. Mass Spectrom.* **2000**, *14*, 772–776.
- (20) Attwood, P. V.; Geeves, M. A. *Anal. Biochem.* **2004**, *334*, 382–389.
- (21) Zechel, D. L.; Konermann, L.; Withers, S. G.; Douglas, D. J. *Biochemistry* **1998**, *37*, 7664–7669.
- (22) Wilson, D. J.; Konermann, L. *Anal. Chem.* **2003**, *75*, 6408–6414.
- (23) Wilson, D. J.; Konermann, L. *Anal. Chem.* **2004**, *76*, 2537–2543.
- (24) Gross, J. W.; Hegeman, A. D.; Vestling, M. M.; Frey, P. A. *Biochemistry* **2000**, *39*, 13633–13640.

- (25) Nichols, K. P.; Gardeniers, H. J. *Anal. Chem.* **2007**, *79*, 8699–8704.
- (26) Nichols, K. P.; Azoz, S.; Gardeniers, H. J. *Anal. Chem.* **2008**, *80*, 8314–8319.
- (27) McLoughlin, S. M.; Kelleher, N. L. *J. Am. Chem. Soc.* **2004**, *126*, 13265–13275.
- (28) McLoughlin, S. M.; Kelleher, N. L. *J. Am. Chem. Soc.* **2005**, *127*, 14984–14985.
- (29) Marshall, A. G.; Hendrickson, C. L.; Jackson, G. S. *Mass Spectrom. Rev.* **1998**, *17*, 1–35.
- (30) Reid, G. E.; McLuckey, S. A. *J. Mass Spectrom.* **2002**, *37*, 663–675.
- (31) Meng, F.; Forbes, A. J.; Miller, L. M.; Kelleher, N. L. *Mass Spectrom. Rev.* **2005**, *24*, 126–134.
- (32) Siuti, N.; Kelleher, N. L. *Nat. Methods* **2007**, *4*, 817–821.
- (33) McLafferty, F. W.; Breuker, K.; Jin, M.; Han, X.; Infusini, G.; Jiang, H.; Kong, X.; Begley, T. P. *FEBS J.* **2007**, *274*, 6256–6268.
- (34) Clarke, D. J.; Mackay, C. L.; Campopiano, D. J.; Langridge-Smith, P.; Brown, A. R. *Biochemistry* **2009**, *48*, 3904–3914.

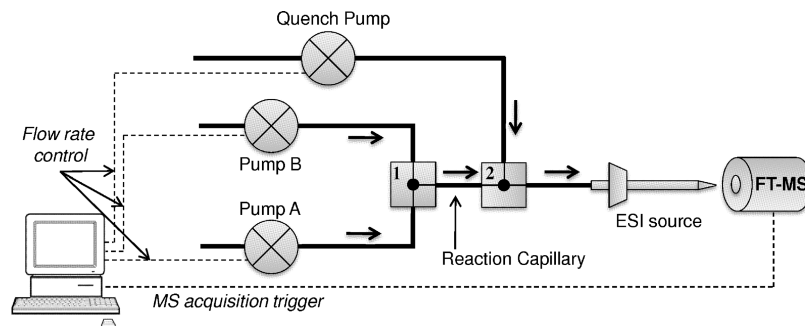


Figure 1. Schematic diagram of the online quench-flow microreactor used for time-resolved ESI-FTICR MS experiments. Pumps A and B deliver a continuous flow of reactants which mix within nanomixer 1. These solutions are allowed to react as they flow through the reaction capillary. In nanomixer 2 a quench solvent is introduced to stop the reaction. The quenched reaction mixture is then connected online to a 12T FTICR MS for analysis. The average reaction time, t , is controlled by varying the flow rates delivered by pumps A and B. Pump flow rates and MS acquisitions are controlled remotely using software written in-house. For further detail see the main text.

EXPERIMENTAL SECTION

Materials. Chymotrypsin and *p*-NPA were purchased from Sigma Chemical Co. (St. Louis, MO). Methanol, water, and formic acid were purchased from Fischer Chemicals (Zurich, Switzerland) and were LC-MS or mass spectrometry grade. Prior to use, chymotrypsin was applied to a PD-Miditrap desalting column (GE Healthcare) and eluted with water.

Apparatus. MilliGAT pumps (Global FIA, Fox Island, WA) were used to deliver solutions with high precision. Nanomixers, fused-silica tubing, Teflon tubing, sleeves, and connectors were purchased from Upchurch Scientific (Oak Harbor, WA). Nanomixers were run using their low back pressure flow path configuration, resulting in an estimated mixing volume of 30 nL.³⁵

Interfacing the Fluids, Mixers, and ESI Sprayer. Reactants were held on ice in 5 mL reservoirs with Teflon tubing leading to Milligat pumps. The pump outlets were connected to nanomixers via fused-silica (100 μm i.d./375 μm o.d.) of 300 mm length (see Figure 1). Reaction capillaries were typically 25 or 75 mm in length and made from fused-silica (50 μm i.d./375 μm o.d.). The outlet of the second nanomixer was connected directly to a standard ESI sprayer (Agilent Technologies, Santa Clara, CA) using fused-silica (100 μm i.d./375 μm o.d.).

Quench-Flow Microreactor Operation. Enzymatic reactions were initiated by mixing chymotrypsin (from pump A) with *p*-NPA (from pump B) in the first nanomixer (see Figure 1). The reaction was allowed to proceed as the mixture flowed through the reaction capillary before being quenched by addition of makeup solvent at the second nanomixer. Therefore, the reaction time was governed by the volume of the reaction capillary and the solution flow rate. For the reaction capillary, 50 μm i.d. silica was employed. Flow rates were varied from 3 to 200 $\mu\text{L min}^{-1}$ in order to produce a range of reaction times from 50 to 5000 ms. During operation, pump A contained 55 μM chymotrypsin in H_2O , and pump B contained *p*-NPA of various concentrations (1–15 mM) in 40% MeOH, pH 8.2. Pump C contained the quench solvent of 99:1 MeOH/formic acid. Pumps A and B were operated at identical flow rates, and the quench pump was operated at a rate equal to the combined rate of A and B.

Software Control. All custom software was written in-house using the Labview visual programming platform (National Instru-

ments; Austin, TX). Briefly, all three milliGAT pumps were controlled from the software via MicroLynx 4 microcontrollers/stepper drivers (Intelligent Motion Systems; Marlborough, CT) and FTICR MS data acquisition was controlled using a contact closure signal to trigger HyStar 3.4 software (Bruker Daltonics, Billerica, MA). A sample table in the controlling software allowed a series of reaction times to be specified, and MS data for each reaction time was collected in an automated fashion. Reaction times were achieved by controlling the flow rate of pumps A and B. After a specified equilibration time delay a trigger was sent to start MS acquisition.

ESI-MS Kinetic Data Collection and Processing. MS acquisitions consisted of 50 scans and were recorded in triplicate for each kinetic time point. This workflow resulted in an “experiment time” (the time taken to collect MS data for a single reaction time point) of approximately 5 min. In order to calculate the ratio of apochymotrypsin to acetylated chymotrypsin (ES’) in each spectra, a variation of the “protein ion relative ratio” (PIRR) system was used.³⁶ Using DataAnalysis software (Bruker Daltonics) each spectrum was background-subtracted. In order to account for all peaks within an isotope cluster, the data was then smoothed using a Gauss algorithm and a window of 0.2 m/z . Within this smoothed spectrum the areas under all 12 charge states, $[\text{M} + 12\text{H}]^{12+}$ to $[\text{M} + 24\text{H}]^{24+}$, were calculated for each species using DataAnalysis software. In order to account for the linear relationship between FTMS detector response and ion charge, these calculated areas were divided by their respective charge states. The resulting charge-normalized areas were combined to give the total area for both the apo and ES’ forms of the enzyme, and the relative ratios of these areas were used for quantitation. The results for each time point were an average of the processed data from the three acquisitions recorded. This lengthy data handling procedure was automated using specifically written software, produced in-house using the Labview visual programming platform (National Instruments; Austin, TX).

FTICR Mass Spectrometry. Mass spectrometry data was acquired on an Apex Ultra Qh-FTICR mass spectrometer equipped with a 12 T superconducting magnet and an electrospray ion source (Bruker Daltonics). Data acquisition was under the control

(35) Bessoth, F. G.; deMillo, A. J.; Manz, A. *Anal. Commun.* **1999**, *36*, 213–215.

(36) Pesavento, J. J.; Mizzen, C. A.; Kelleher, N. L. *Anal. Chem.* **2006**, *78*, 4271–4280.

of HyStar 3.4 software (Bruker Daltonics). Desolvated ions were transmitted to a 6 cm Infinity cell penning trap. Trapped ions were excited (frequency chirp 48–500 kHz at 100 steps of 25 μ s) and detected between m/z 600 and 3000 for 0.5 s to yield a broadband 512K time-domain transient. Each spectrum was the sum of 50 mass analyses. The mass spectra were externally calibrated using ES tuning mix (Agilent) and analyzed using DataAnalysis software (Bruker Daltonics).

Isotopic Fitting. Isotope distributions of specific charge states were predicted using IsotopePattern software (Bruker Daltonics) from theoretical empirical formulas. These were overlaid upon the recorded experimental data as scatter plots, with the theoretical apex of each isotope peak designated by a circle.

Top-Down Fragmentation. Top-down fragmentation was performed on the 12T Qh-FTICR. First, a specific ion species was isolated using the mass-resolving quadrupole, and MS/MS was performed using collision-induced dissociation (CID) or electron capture dissociation (ECD). For CID, the collision voltage was typically set between 20 and 35 V. For ECD, 1.8 A was applied to the dispenser cathode filament (Heatwave Technologies), 20 V to the lens, 0.8 V to the bias, and a pulse of between 5 and 14 ms was employed. Fragmentation data was the sum of 250–750 acquisitions, and data analyses were performed using DataAnalysis (Bruker Daltonics). The SNAP 2.0 algorithm was used for automated peak picking; monoisotopic mass-to-charge ratios calculated using this process are highlighted in the text preceded by a prime symbol (\prime). The resulting top-down fragment mass lists were searched against the primary sequence of each polypeptide chain in mature chymotrypsin using BioTools 3.0 (Bruker Daltonics) and ProSight-PTM software packages.^{37,38} Mass error tolerances were set for all searches at 10 ppm.

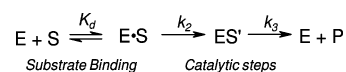
DATA ANALYSIS

Traditional rapid mixing continuous flow systems are operated under turbulent flow conditions, with constant mixing between fast and slow regions within the apparatus. However, turbulent flow cannot normally be achieved for miniaturized online ESI-MS experiments, and these systems operate in the laminar flow regime.³⁹ The resulting parabolic velocity profiles associated with laminar flow act to distort the measured kinetics and were thought to prevent accurate data collection. However, recent computer simulations and experimental studies by Konermann and co-workers have shown that this “blurring” is reduced by the counteracting effects of molecular diffusion.^{22,39} This research group has developed a theoretical framework for performing kinetic calculations which takes into account laminar flow effects, and they have clearly demonstrated the feasibility of performing kinetic studies in this flow regime. Indeed, they successfully monitor the pre-steady-state kinetic of chymotrypsin under laminar flow conditions.²³ To validate our quench-flow system we have studied the same enzymatic reaction, and have employed the same theoretical framework in our data analysis.

During the catalytic cycle of the protease chymotrypsin, Ser₁₉₅ acts as a reactive nucleophile and can attack both amine and

ester bonds. Ser₁₉₅ forms a covalent bond with the carbonyl carbon of *p*-NPA—acetylating the active residue ($\Delta m + 42$ Da) and releasing the hydrolysis product *p*-nitrophenol. The enzyme-bound acyl-intermediate, ES', is subsequently hydrolyzed by water, regenerating the free enzyme. The accepted kinetic mechanism for the reaction is shown in Scheme 1. Briefly, there is an initial noncovalent association between the enzyme and the *p*-NPA substrate, forming E·S, followed by nucleophilic attack by Ser₁₉₅ resulting in acetylation and formation of the acylated serine intermediate, ES'. Finally, hydrolysis of this intermediate occurs resulting in the free enzyme (E) and releasing the product, acetate (P).

Scheme 1



Pre-steady-state kinetic theory states that

$$k_{\text{obs}} = k_3 + k_2[\text{S}]/(K_d + [\text{S}]) \quad (2)$$

where [S] is the concentration of substrate.⁴⁰ Therefore, measurements of k_{obs} as a function of [S] allow the determination of K_d , k_2 , and k_3 .⁴⁰

RESULTS AND DISCUSSION

Pre-Steady-State Kinetic Analysis of *p*-NPA Hydrolysis by Chymotrypsin. The chymotrypsin-catalyzed hydrolysis of *p*-NPA was chosen to validate our quench-flow FTMS system, as this reaction has been extensively studied, using both MS- and optical-based detection techniques.^{23,41} The flow rates of pumps A and B were systematically altered to produce quenched reactions at various time points, and for each time point three ESI mass spectra were recorded (see the Experimental Section). The pump flow rates and MS acquisitions were controlled via custom software, which allowed kinetic data to be collected in a semiautomated manner. Using a fixed concentration of *p*-NPA, spectra for 15 different reaction time points could be collected in approximately 150 min. It is worth noting that the speed of data acquisition is governed by the scan speed of the mass spectrometer. The 500 ms acquisition speed utilized in FTICR MS is relatively slow, and by using a faster scanning instrument quench-flow data acquisition time could be dramatically decreased. Typical spectra, recorded using our quench-flow FTMS setup, are shown in Figure 2. Figure 2A shows the charge state distribution in a typical spectrum; species corresponding to the $[\text{M} + 12\text{H}]^{12+}$ to $[\text{M} + 24\text{H}]^{24+}$ charge states of chymotrypsin were observed, and the spectrum is consistent with that of a denatured protein. Analysis of the isotopic distribution of the $[\text{M} + 20\text{H}]^{20+}$ charge state revealed that the mass of chymotrypsin used in this study was consistent with the δ' -form of the enzyme (Figure 2, parts B and C top, theoretical empirical formula $[\text{C}_{1118}\text{H}_{1780}\text{N}_{302}\text{O}_{352}\text{S}_{12}]^{20+}$; red circles). The change in the abundance of the $[\text{M} + 20\text{H}]^{20+}$ charge state of chymotrypsin observed after reacting the enzyme with 2.5

(37) LeDuc, R. D.; Taylor, G. K.; Kim, Y. B.; Januszzyk, T. E.; Bynum, L. H.; Sola, J. V.; Garavelli, J. S.; Kelleher, N. L. *Nucleic Acids Res.* **2004**, *32*, W340–W345.

(38) Leduc, R. D.; Kelleher, N. L. *Curr. Protoc. Bioinf.* **2007**, Unit 13 16.

(39) Konermann, L. *J. Phys. Chem. A* **1999**, *103*, 7210–7216.

(40) Price, N. C.; Stevens, L. *Fundamentals of Enzymology: Cell and Molecular Biology of Catalytic Proteins*, 3rd ed.; OUP: Oxford, U.K., 1999.

(41) Gutfreund, H.; Sturtevant, J. M. *Biochem. J.* **1956**, *63*, 656–661.

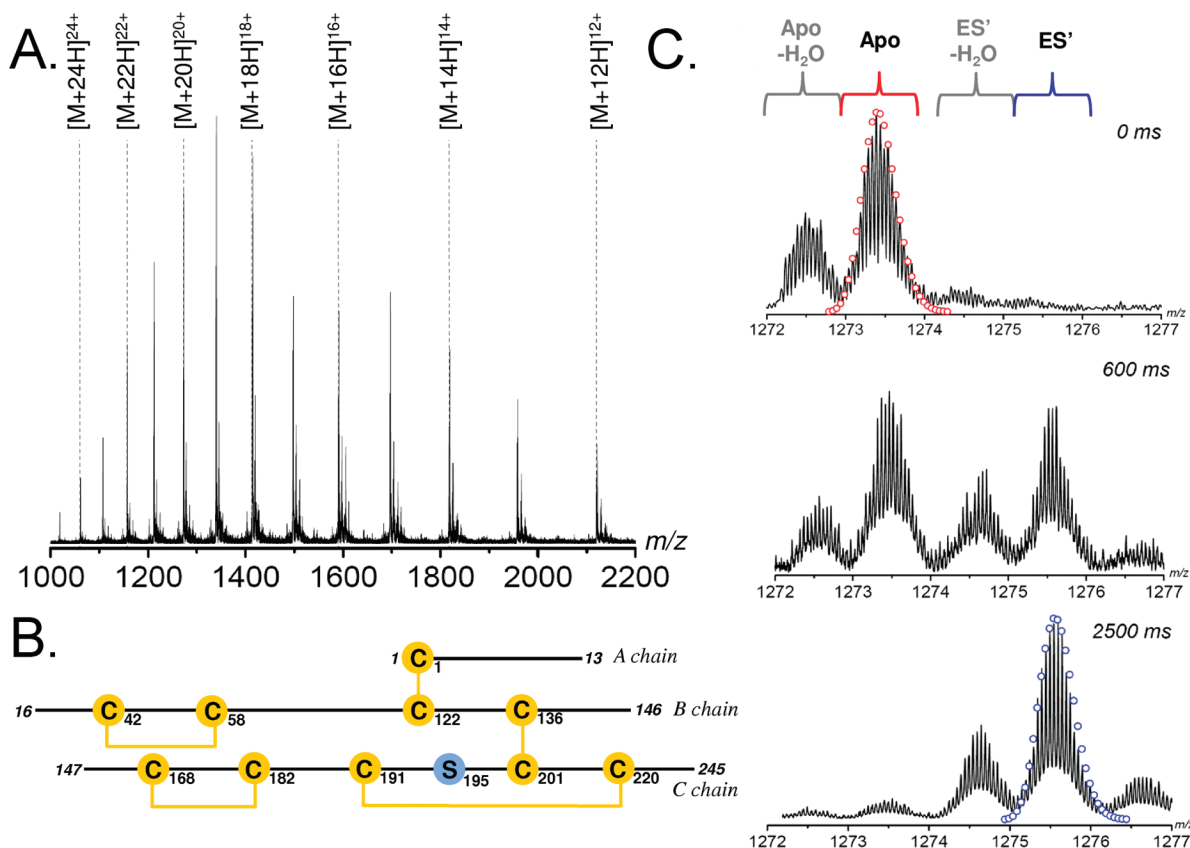


Figure 2. (A) Typical ESI-FTICR mass spectrum for chymotrypsin acquired using the online rapid-quench microreactor. Each charge state is annotated. (B) Schematic representation of the primary structure of δ' -chymotrypsin which comprises three polypeptide chains (A, B, and C) linked by two intermolecular disulfide bonds. Disulfide bonds are highlighted in yellow, and the active site, Ser₁₉₅, is highlighted in blue. Numbering is consistent with the primary sequence of bovine chymotrypsin A (EC 3.4.21.1). (C) High-resolution spectra of the $[M + 20H]^{20+}$ charge state of δ' -chymotrypsin during the pre-steady-state hydrolysis of *p*-NPA. Spectra were recorded at reaction times 0 (top), 600 (middle), and 2500 (bottom) ms, using 2.5 mM *p*-NPA. The theoretical isotope distribution of unmodified (apo) chymotrypsin is shown as a scatter plot in red, and the theoretical isotope distribution of the acetylated form of chymotrypsin (ES'; $\Delta\text{mass} + C_2H_2O$) is shown in blue. A species with a mass consistent with loss of H₂O from the protein was also observed under all conditions studied.

mM *p*-NPA for 600 and 2500 ms is shown in Figure 2C. Over time it is clear that a second species, with a Δmass of +42 Da, accumulates in the spectrum. This species has an isotope distribution consistent with δ' -chymotrypsin with the addition of a single acetyl group (Figure 2C bottom, theoretical empirical formula $[C_{1120}H_{1782}N_{302}O_{353}S_{12}]^{20+}$; blue circles), this is assigned as the pre-steady-state accumulation of the ES' covalent intermediate. After 600 ms both the unmodified (apo) form of the enzyme and the covalent complex (ES') are present, and by 2500 ms the ES' complex has become the dominant species in the spectrum.

In order to convert the spectra recorded at each reaction time point into quantitative data suitable for kinetic analysis, a system based upon PIRR was used (see the Experimental Section). This analysis assumes that the ionization efficiency of the apo and ES' forms of chymotrypsin are equal. For quantitative analysis of modified proteins (>10 kDa), previous reports have demonstrated that such an assumption is precise to ~5%.^{42,43} Indeed, preliminary experiments demonstrated that the ionization efficiencies of apo and ES'-chymotrypsin are similar to ~4% (data not shown). In

order to take into account this uncertainty during the calculation of the kinetic parameters, an intrinsic error of 5% was included with each value of k_{obs} .

Figure 3A shows the pre-steady-state buildup of the ES' intermediate species over time for four different concentrations of *p*-NPA. The data was fitted to eq 3

$$[ES'](t) = C\{1 - \exp(-k_{\text{obs}}t)\} \quad (3)$$

which provided an observed rate constant, k_{obs} , for each concentration of *p*-NPA.¹⁹ In total, kinetic data was collected for 10 different concentrations of the substrate. These k_{obs} values were subsequently plotted as a function of substrate concentration and, on the basis of eq 2, this data allowed the determination of the kinetic constant of K_d , k_2 , and k_3 (see Figure 3B). The values obtained for K_d , k_2 , and k_3 are 1.6 ± 0.3 mM, 2.8 ± 0.2 s⁻¹, and 0.0 ± 0.2 s⁻¹, respectively. It is clear that the value of k_3 is too small to accurately determine using this approach, as found in the MS-based kinetic study performed by Wilson and Konermann.²³ This is not wholly surprising, as k_3 must be much smaller than k_2 for pre-steady-state buildup of ES'. Thus, k_3 is the rate-determining step and can be approximated as k_{cat} , which can be calculated by kinetic analysis in the steady-state regime. The values of k_2 and K_d reported here are in good

(42) Gordon, E. F.; Mansoori, B. A.; Carroll, C. F.; Muddiman, D. C. *J. Mass Spectrom.* **1999**, *34*, 1055–1062.

(43) Hicks, L. M.; O'Connor, S. E.; Mazur, M. T.; Walsh, C. T.; Kelleher, N. L. *Chem. Biol.* **2004**, *11*, 327–335.

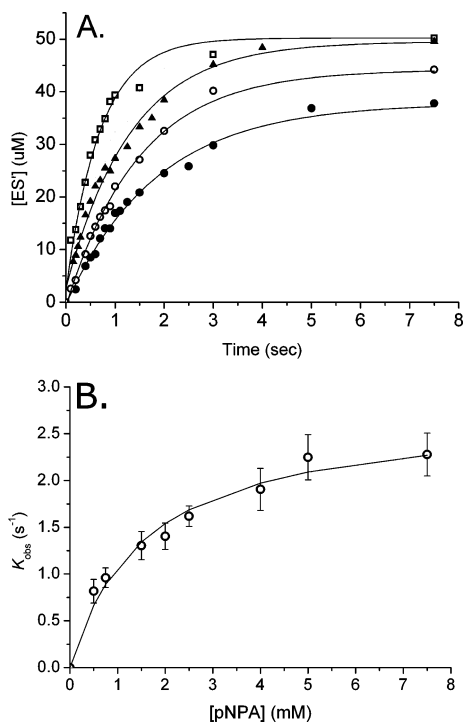


Figure 3. Pre-steady-state kinetic analysis of the hydrolysis of *p*-NPA by chymotrypsin. (A) The accumulation of the ES' covalent complex over time for different concentrations of *p*-NPA (closed circles, 0.5 mM; open circles, 0.75 mM; closed triangles, 2 mM; open squares, 5 mM). The data was obtained by calculating the area under the 12 most abundant charge states for the unmodified (E) and intermediate-bound (ES') forms of chymotrypsin. Each data point is an average calculated concentration obtained from three independent MS acquisitions. Data points were fitted to eq 3 to provide k_{obs} . (B) Measured values of k_{obs} as a function of *p*-NPA concentration. The error bars represent the error calculated from the fits to the concentration time profiles for the ES' complex shown in panel A. The solid line represents a fit of these k_{obs} values based on eq 2 and provides values for K_d , k_2 , and k_3 .

agreement with the values previously reported for δ' -chymotrypsin by Wilson and Konermann of 1.7 ± 0.2 mM and 3.7 ± 0.3 s⁻¹ using an MS-based approach, and 1.6 ± 0.1 mM and 3.6 ± 0.2 s⁻¹ using optical detection.²³

The above results clearly demonstrate the feasibility of using this automated quench-flow FTMS approach for pre-steady-state enzyme kinetic analysis and add credence to the viability of previously published MS-based kinetic studies.^{18,20,21,23} To our knowledge, this work represents the first reported use of online quench-flow coupled with FTICR MS.

Analysis of the ES' Complex by Top-Down Tandem Mass Spectrometry. Interfacing a quench-flow microreactor with FTICR MS allows direct interrogation of covalently bound enzyme intermediates by a variety of top-down fragmentation techniques. Top-down fragmentation involves the intact mass measurement of a protein and dissociation of the intact protein to produce tandem mass spectrometry data. This can be used to determine the primary structure of the molecule and locate modified amino acids. The importance of high-resolution data sets and high mass accuracy for successful top-down analysis is well-documented, and FTICR mass analysers are unsurpassed in these respects.^{29,44,45}

Successful, top-down fragmentation of the ES' complex would allow the nature of the quenched intermediate and the position of the catalytic residue in the polypeptide chain to be deduced, thus providing valuable insight into the chemical mechanism of enzymatic catalysis.

The "online" quench-flow MS apparatus used in this work prohibited derivatization of the quenched ES' complex before MS analysis. Therefore, reduction and alkylation of the quenched intermediate was not possible prior to MS analysis, and top-down fragmentation had to be conducted on the fully oxidized δ' -chymotrypsin molecule. Traditionally, the presence of disulfide bonds is seen as a hindrance to tandem MS as the presence of intramolecular disulfide bridges can limit protein fragmentation and reduce the available sequence information.^{46,47} Indeed, our initial top-down experiments, using both CID and infrared multiphoton dissociation (IRMPD), resulted in no detectable cleavage of either the inter- or intramolecular disulfide linkages within chymotrypsin (data not shown). Consequently, after data analysis, the assigned fragments from these tandem MS experiments were limited to *b*-ions derived from the N-terminus of the B and C chains (data not shown). Not a single cleavage could be identified from within the region of the C chain containing the catalytic serine (Ser₁₉₅), which is situated within a loop formed by an intramolecular disulfide bond between Cys₁₉₁ and Cys₂₀₁ (see Figure 2B).

Since its introduction in 1998,⁴⁸ ECD has been recognized as a powerful technique for top-down tandem MS.^{49,50} ECD has garnered significant interest due to its tendency to retain post-translational and chemical modifications, resulting in more extensive sequence coverage when compared to other fragmentation techniques.^{51,52} Furthermore, with the development of activated ion (AI) ECD, the utility of this fragmentation technique has been extended to larger proteins, and top-down analysis of proteins up to 45 kDa has been reported.^{53,54} One other unique feature of ECD is that it can efficiently cleave disulfide bonds, presumably due to the S-S bond's high hydrogen atom affinity.⁵⁵ Various groups have reported that ECD (or AI ECD) can be used to obtain sequence information of disulfide-rich peptides, for example, the

- (44) Nielsen, P. F.; Roepstorff, P.; Clausen, I. G.; Jensen, E. B.; Jonassen, I.; Svendsen, A.; Balschmidt, P.; Hansen, F. B. *Protein Eng.* **1989**, *2*, 449–457.
- (45) Henry, K. D.; Williams, E. R.; Wang, B. H.; McLafferty, F. W.; Shabanowitz, J.; Hunt, D. F. *Proc. Natl. Acad. Sci. U.S.A.* **1989**, *86*, 9075–9078.
- (46) Speir, J. P.; Senko, M. W.; Little, D. P.; Loo, J. A.; McLafferty, F. W. *J. Mass Spectrom.* **1995**, *30*, 39–42.
- (47) Loo, J. A.; Edmonds, C. G.; Udseth, H. R.; Smith, R. D. *Anal. Chem.* **1990**, *62*, 693–698.
- (48) Zubarev, R. A.; Kelleher, N. L.; McLafferty, F. W. *J. Am. Chem. Soc.* **1998**, *120*, 3265–3266.
- (49) Zubarev, R. A. *Curr. Opin. Biotechnol.* **2004**, *15*, 12–16.
- (50) Cooper, H. J.; Hakansson, K.; Marshall, A. G. *Mass Spectrom. Rev.* **2005**, *24*, 201–222.
- (51) Zubarev, R. A.; Horn, D. M.; Fridriksson, E. K.; Kelleher, N. L.; Kruger, N. A.; Lewis, M. A.; Carpenter, B. K.; McLafferty, F. W. *Anal. Chem.* **2000**, *72*, 563–573.
- (52) Haselmann, K. F.; Jorgensen, T. J.; Budnik, B. A.; Jensen, F.; Zubarev, R. A. *Rapid Commun. Mass Spectrom.* **2002**, *16*, 2260–2265.
- (53) Horn, D. M.; Ge, Y.; McLafferty, F. W. *Anal. Chem.* **2000**, *72*, 4778–4784.
- (54) Ge, Y.; Lawhorn, B. G.; ElNaggar, M.; Strauss, E.; Park, J. H.; Begley, T. P.; McLafferty, F. W. *J. Am. Chem. Soc.* **2002**, *124*, 672–678.
- (55) Zubarev, R. A.; Kruger, N. A.; Fridriksson, E. K.; Kelleher, N. L.; Lewis, M. A.; Horn, D. M.; Carpenter, B. K.; McLafferty, F. W. *J. Am. Chem. Soc.* **1999**, *121*, 2857–2862.

analysis of the defensin class of antimicrobial peptides.^{56,57} It is interesting to note that, to obtain sequence coverage from a region of protein sequence within a disulfide bond, two cleavages must take place—cleavage of the disulfide bond and amide backbone cleavage.

The ES' complex of chymotrypsin and 3 mM *p*-NPA was generated by using the online rapid-quench microreactor attached to the 12 T FTICR MS, with the microreactor set to produce a quench reaction time of $t = 2000$ ms. At this reaction time the ES' complex was the dominant species in the mass spectrum and displayed an isotope distribution consistent with the δ' -isoform of chymotrypsin + C₂H₂O. Five charge states ([M + 17H]¹⁷⁺ to [M + 21H]²¹⁺) of the ES' species were systematically isolated and subjected to fragmentation using ECD. A typical ECD spectrum is shown in Figure 4A. Application of a collision voltage of between 5 and 10 V to the collision cell prior to ECD was found to produce more extensive fragmentation, presumably through an ion-activated process. All ES' charge states dissociated by ECD resulted in two dominant fragment ions. The first, a singly charged species, with monoisotopic m/z 1253.6855 (Figure 4A, green diamond) was consistent with the A chain of chymotrypsin, formed by cleavage of the disulfide linkage between Cys₁ and Cys₁₂₂ and with addition of an H atom to the fragment (predicted isotope distribution [C₅₆H₉₇N₁₄O₁₆S₁]¹⁺; green circles). The second species displayed charge states of [M + 4H]⁴⁺, [M + 5H]⁵⁺, and [M + 6H]⁶⁺ (Figure 4A, red diamonds), the [M + 6H]⁶⁺ species displaying monoisotopic m/z 1720.0040. Isotope modeling of this species was consistent with the acylated C chain of chymotrypsin formed by cleavage of the intermolecular disulfide between Cys₁₃₆ and Cys₂₀₁, and suggests that the species retained the two C chain intramolecular disulfide bridges, and occurs with addition of an H atom to the fragment (predicated isotope distribution [C₄₄₆H₇₁₈N₁₂₆O₁₄₁S₇]⁶⁺; red circles). ECD-induced disulfide bond cleavage is thought to proceed via capture of a hydrogen atom, producing an even-electron reduced cysteine (Cys–SH) and an odd-electron cysteine radical (Cys–S•). It is interesting to note that the two major fragments observed in the ECD of chymotrypsin occurred with retention of the neutralized H atom, a phenomenon also observed by Zubarev et al.⁵⁵

In addition to these two dominant species, extensive further fragmentation was observed for all the charge states studied (see Figure 4A, highlighted in blue; Figure 4B). Fragment mass lists were assembled using DataAnalysis (Bruker Daltonics), and these were searched using BioTools 3.0 (Bruker Daltonics) and ProSight-PTM software packages. After disulfide bond cleavage by ECD, one of the two cysteine residues increases in mass by 1 Da (the consequence of H atom capture). In order to take this into consideration during data analysis, the redox states of all 10 cysteine residues were designated as oxidized, and variable modifications of an additional H atom were specified for each. In total 177 fragments were assigned—5 derived from the A chain, 138 derived from the B Chain, and 34 derived from the C chain

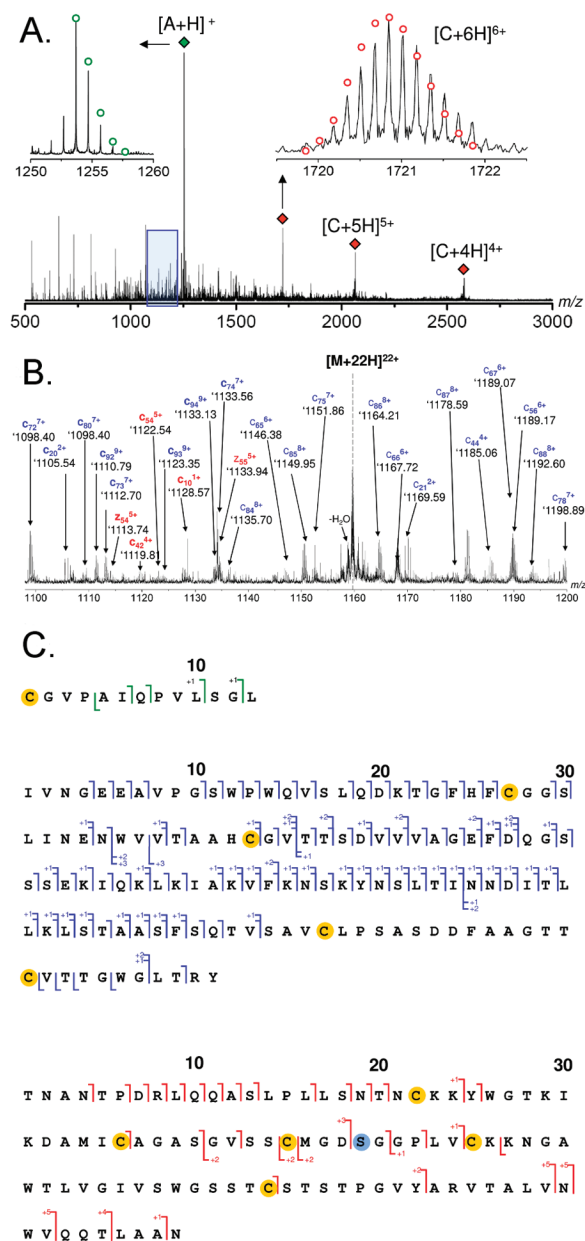


Figure 4. Analysis of the enzyme-bound acyl-intermediate of δ' -chymotrypsin by top-down fragmentation using electron capture dissociation. (A) The mass spectrum obtained after ECD of the [M + 22H]²²⁺ charge state (m/z 1160) of the ES' covalent complex. Two dominant species are observed—the A chain (green diamond) and C chain (red diamonds) of chymotrypsin formed by cleavage of the two intermolecular disulfide bonds. Extensive further fragmentation was also observed. The area of the spectra highlighted in blue is shown in panel B. (B) The m/z range of 1100–1200 with assigned ECD fragments. Fragments annotated in blue originate from the B chain; fragments annotated in red originate from the C chain. (C) ECD cleavage maps of the A, B, and C chains of chymotrypsin (combined for all charge states studied). The cysteine residues are highlighted in yellow; the acetylated Ser₁₉₅ in chain C is highlighted in blue. Fragments containing additional H atoms, as a consequence of ECD fragmentation of a disulfide bond, are signified by +1, +2, +3 on the cleavage maps.

(see Figure 4C). Interestingly, many of these fragments are the result of two bond cleavages (one disulfide and one backbone amide cleavage) and, in some cases, three bond cleavages (two disulfide cleavages and a backbone amide cleavage). Fragmenta-

(56) Campopiano, D. J.; Clarke, D. J.; Polfer, N. C.; Barran, P. E.; Langley, R. J.; Govan, J. R.; Maxwell, A.; Dorin, J. R. *J. Biol. Chem.* **2004**, *279*, 48671–48679.

(57) Tsybin, Y. O.; Witt, M.; Baykut, G.; Kjeldsen, F.; Hakansson, P. *Rapid Commun. Mass Spectrom.* **2003**, *17*, 1759–1768.

tion of the C chain includes a series of both *c* and *z* ions from the region between Cys₁₉₁ and Cys₂₀₁. Fragments containing the acetylated group allow the catalytic amino acid to be pinpointed to a five amino acid containing region (₁₉₂MGDSG₁₉₆), and the unacylated *c*₄₈ ion suggests that the modification is limited to the dipeptide (₁₉₅SG₁₉₆).

CONCLUSION

We have developed a semiautomated quench-flow microreactor which is compatible with ESI mass spectrometry for kinetics measurements. Reaction time is governed by flow rate though a fixed volume capillary, and software written in-house is used to control the device and for synchronized MS data acquisition. We have interfaced the microreactor with a 12T FTICR MS in order to monitor the accumulation of a transient covalent acyl enzyme intermediate over time and have demonstrated that this system can produce accurate pre-steady-state kinetic data.

By using the FTMS instrument as the detector, we were able to utilize the top-down fragmentation capabilities of the instrument to interrogate the quenched enzyme intermediate. Using ECD we demonstrated the power of this approach by locating the transient modification to a five amino acid section within the 250 amino

acid enzyme. It is easy to envisage how the top-down experimental approach used here could be employed to locate key residues involved in the catalytic cycles of a variety of enzymes.

This study highlights the power of using FTICR in enzyme analysis. The approach described above can yield valuable information into both the kinetic mechanism of enzyme mechanisms, providing kinetic parameters using unlabeled substrates, as well as significant insight into the chemical mechanism of enzyme catalysis, by the identification of the nature and location of enzyme-bound intermediates.

ACKNOWLEDGMENT

This work has been supported by the RASOR consortium (Grant from the Biotechnology and Biological Sciences Research Council (BB/C511599/1)) and The University of Edinburgh. We also thank Professor Neil Kelleher for the use of ProSight-PTM software.

Received for review November 17, 2009. Accepted January 14, 2010.

AC9026302